CALIFORNIA INSTITUTE OF TECHNOLOGY

ELECTRON TUBE AND MICROWAVE LABORATORY

BEHAVIOR OF TRAVELING-WAVE TUBES NEAR CIRCUIT CUTOFF

by

Daniel G. Dow

TECHNICAL REPORT NO. 10

February 1959

A REPORT ON RESEARCH CONDUCTED UNDER

CONTRACT WITH THE OFFICE OF NAVAL RESEARCH

BEHAVIOR OF TRAVELING-WAVE TUBES NEAR CIRCUIT CUTOFF

by

Daniel G. Dow

Technical Report 10

CALIFORNIA INSTITUTE OF TECHNOLOGY

Pasadena, California

A Technical Report to the Office of Naval Research

Contract Nonr 220(13)

February 1959

BEHAVIOR OF TRAVELING-WAVE TUBES NEAR CIRCUIT CUTOFF

D. G. Dow

ABSTRACT

A theory is developed which explains the operation of a traveling wave tube when operated near the cutoff frequency of the slow wave circuit, including the effect of two circuit waves instead of the usual one. The theory is normalized in a manner analogous to that used in more conventional analyses, making a relatively small number of curves applicable to a large number of cases. The relationship between this theory and the three-wave theory usually used in traveling-wave tube analysis is shown, and they are in agreement when the system is operated far from the cutoff frequency. Numerical results are given for a range of parameters which might be useful in traveling wave tube design, and an excellent agreement with published experimental results is shown.

BEHAVIOR OF TRAVELING-WAVE TUBES NEAR CIRCUIT CUTOFF

1. Introduction

The conventional analysis of the traveling wave amplifier (or oscillator) assumes a slow wave circuit with only one space harmonic which is capable of interacting with the electron beam. In actual fact, any useful slow wave circuit has an infinite number of space harmonics which may be capable of interaction with the beam. It is normally assumed that only one of these at a time will be of any interest, and this is usually the case.

There is one example, however, in which the presence of two circuit waves is extremely important. This occurs when the frequency is adjusted so that the tube operates right at the edge of a pass band. At this point, there will be two space harmonics of approximately equal importance, and the analysis of interaction will necessarily require four characteristic waves (two from the circuit and two from the beam) instead of the usual three. This paper will present an analysis of a particular circuit model which exhibits the features described, and shows the relationship with the simpler three-wave theory. In addition, the theory is normalized in a manner analogous to that used by Pierce for the three-wave case, so that the numerical results obtained can be applied with some generality.

It should be pointed out that this type of analysis is not new in principle. Reutz[1] and Gould[2] have used methods similar to the

ones used here, but in each case they treated only very specialized circuit models. By an appropriate normalization in the present paper, we have generalized the results a great deal, with, of course, a certain loss in accuracy.

This paper was initially motivated by a particular application; the suppression of backward-wave oscillation. It has been shown that a stop band can be deliberately used in a helix[3] (or other slow wave circuit) in order to prevent backward wave oscillations which would otherwise appear. While this technique is known to work empirically, it has never been explained quantitatively to the author's knowledge, except for the one case worked out by Gould.

In order to analyze this problem, it must first be recognized that the basic source of space harmonics is the periodicity of the circuit. In other words, the basic feature of the analysis will be the inclusion of the periodic nature of the circuit. It is most convenient mathematically to do this using a particular model, but it will be shown that the results apply at least to two cases which might represent two types of traveling wave tubes. Using the particular model, a periodic traveling wave tube will be analyzed and numerical data presented for the conditions of start oscillation in a backward wave oscillator.

2. Basic Analysis of a Periodic Traveling Wave Tube

a) The circuit equation. Since this problem was originally motivated by the filter helix method of oscillation suppression, a loaded transmission line equivalent circuit will be used to derive

the applicable circuit equation. A number of equivalent circuits can be made to give approximately the same final result, but in an exact analysis the form of the equivalent circuit is important. Reutz[1] has investigated some of the consequences of this for a particular class of equivalent circuits.

The circuit model used is shown in Figure 1. One might speculate whether it is more reasonable to have the beam interact with the voltage across a shunt element or a series element. The shunt element has been chosen for this analysis, while the use of voltage across the series element would result in a factor $1/4 \sin^2 \theta/2$ in the coupling impedance (right side of equations 8, 13, 14, 32, 33, 38, and 40) and no other change. One can estimate which to use in any physical situation by studying the case $\theta = 0$. If longitudinal field exists at the beam when $\theta = 0$, the equations should be used as they stand. If no such field exists, the $1/4 \sin^2 \theta/2$ factor may be used as indicated above.

For the circuit shown in Figure 1, the a.c. current in the electron stream is denoted by i_1, and is assumed to interact with the circuit through narrow gaps connected to the circuit. These gaps are assumed to have no capacitance. The relationship between this model and a more physical model of a helix is basically a modification of the effective interaction impedance. It appears most straightforward to use the model of Figure 1, converting to a more physical model through the use of the effective coupling impedance later.

The circuit itself is considered to be a transmission line of characteristic admittance Y_o, and with a phase shift per section of

θ_o . This transmission line is loaded periodically by shunt admittances of value Y . It is assumed that these admittances are connected at the same point that the current flows into the circuit from the beam. This restriction can be removed if necessary, through use of the coupling impedance concept. Since the circuit is periodic it will be assumed that all quantities change by a multiplicative factor $e^{-j\theta}$ when the signal advances one section of the circuit. Thus the phase shift per section is θ which may be a complex number in the presence of the beam or loss. With these definitions, and those apparent from the figure, the following equations can be written among the variables.

$$i_3 = -j\, Y_o \cot \theta_o\, V + j\, Y_o \csc \theta_o\, e^{-j\theta}\, V \qquad (1)$$

$$i_4 = -j\, Y_o \csc \theta_o\, V + j\, Y \cot \theta_o\, e^{-j\theta}\, V \qquad (2)$$

$$i_2 = Y\, V \qquad (3)$$

$$i_1 = (i_3 + i_2 - i_4) \qquad (4)$$

These reduce eventually to Eq. 5 relating i_1 and V , the circuit voltage at the reference point.

$$\frac{i_1}{V} = -j\, 2Y_o \csc \theta_o \left[\cos \theta_o + j \frac{Y}{2Y_o} \sin \theta_o - \cos \theta\right] \qquad (5)$$

If there were no beam present, that is, $i_1 = 0$, the circuit would have a phase shift per section θ_1 , which will be called the cold circuit phase shift. Since this is usually a measurable quantity, while θ_o is not, it is preferable to express Eq. 5 in terms

of this quantity, and the resulting circuit equation which will be used is given in Eq. 6 .

$$\frac{i_1}{V} = -j\, 2Y_o \csc \theta_o \left[\cos \theta_1 - \cos \theta\right] \tag{6}$$

b) Electronic equation. Since the beam sees exactly the environment which was used by Gould[2], the same electronic equations may be used. Converting the matrix notation used in his results to the direct physical quantities, results in Eq. 7 describing the effect of a circuit voltage V on the beam current i_1 . In this equation the following new variables have been used:

$$\theta_e = \frac{\omega}{u_o}\mathcal{L} \qquad \text{and} \qquad \theta_q = \frac{\omega_q}{u_o}\mathcal{L}$$

where u_o = d.c. beam velocity
ω = signal radian frequency
ω_q = reduced plasma frequency for the beam
I_o = d.c. beam current
V_o = d.c. beam voltage

$$\frac{i_1}{V} = -j \frac{\frac{I_o}{2V_o} e^{-j\theta_e} \frac{\theta_e}{\theta_q} \sin \theta_q}{e^{-j(\theta+\theta_e)} \left[-4 \sin^2 \left(\frac{\theta-\theta_e}{2}\right) + 2(1-\cos \theta_q)\right]} \tag{7}$$

If there is no circuit present, that is, $V = 0$, the denominator of the right side of (7) must vanish, and this will give the correct result for space charge waves in a drift region.

c) Characteristic equation. To find the characteristic waves of the system, the circuit admittance, Eq. 6, must be equated

to the beam admittance, Eq. 7. The result of this is given in Eq. 8 which is a transcendental equation for the various allowed values of θ . If this equation could be solved, it would give all of the characteristic waves of the system consisting of a beam (with two space charge waves) coupled to the circuit (with an infinite number of space harmonics)

$$(\cos\theta - \cos\theta_1)\left[4\sin^2\left(\frac{\theta-\theta_e}{2}\right) - 2(1-\cos\theta_q)\right] = -\frac{I_o}{4Y_oV_o}\sin\theta_o\,\theta_e\,\frac{\sin\theta_q}{\theta_q} \qquad (8)$$

Fortunately, it will not be necessary to attempt the solution of this equation, since we are interested in the system behavior when the beam is approximately synchronized with a space harmonic, or at most with two of them. The condition to be investigated in detail is indicated in Fig. 2 where one forward space harmonic and one backward space harmonic are coupled together to create a cutoff frequency, and the electron beam velocity is near to the velocity of these two space harmonics. It is well known that the effect of the beam is negligible unless it does have approximately the same velocity as a circuit wave.

The relationship between this equation and the standard characteristic equations for forward and backward wave tubes will be demonstrated later. For the present, let us assume--in accordance with Fig. 2--that θ, θ_e , and θ_1 are all close to π . The following definitions will be used, where F is a constant to be determined later.

$$\theta = \pi + Fx \tag{9}$$

$$\theta_e = \pi + Fb_e \tag{10}$$

$$\theta_1 = \pi + Fb_1 \tag{11}$$

$$\theta_q = Fb_q \tag{12}$$

Using these definitions, and the assumption that all of the deviations from π are small, the trigonometric functions can be expanded, resulting in Eq. 13.

$$\frac{F^4}{2}(x^2 - b_1^2)\left[(x - b_e)^2 - b_q^2\right] = \frac{I_o}{4Y_oV_o}\sin\theta_o(\pi + Fb_e)\frac{\sin\theta_q}{\theta_q} \tag{13}$$

Since F has not yet been fixed, it seems reasonable to let the terms in the equation for x be independent of current, voltage, and other quantities on the right side of (13). This results in the definition

$$F^4 = \frac{I_o}{2Y_oV_o}\pi\sin\theta_o\frac{\sin\theta_q}{\theta_q} \quad . \tag{14}$$

Furthermore, on the right side of (13), the quantity F^4 will usually be small and thus we shall neglect, as being of second order in small quantities, the term involving F in $(\pi + Fb_e)$. The resulting characteristic equation is a fairly simple quartic in x as given in Eq. 15. The roots of this equation will give the four values of allowed propagation constant.

$$(x^2 - b_1^2)\left[(x - b_e)^2 - b_q^2\right] - 1 = 0 \tag{15}$$

It is interesting to consider physically the effect of these approximations. The initial characteristic equation, (8), accounts for all waves and all space harmonics. The traditional approach using a smooth transmission line would result if we assumed all phase shifts to be small and expanded about $\theta = 0$. This would result in an equation with two basic circuit waves, but no space harmonics. When the smooth circuit approach is used, it is easy to show as Pierce[4] does, that if one of the circuit waves is coupled to the electron beam, the other one is essentially unperturbed by it. This demonstration would hold for the backward traveling fundamental of our present circuit also, but is not true for our first backward space harmonic. By expanding all phase shifts about π, we have kept only the forward fundamental, and the first backward space harmonic. We have neglected all of the circuit space harmonics which are not synchronous with the beam, and are left with a four-wave system instead of the traditional three-wave one.

d) Boundary conditions. In order to complete the solution, the effect of the boundary conditions must be included. The model of Fig. 1 shows the circuit boundary conditions which are assumed. In the general case, a current generator and terminating admittance are connected at each end, so that input signals may be sent in either direction along the circuit. In any particular case, of course, at least one of the generators will be absent; however, the boundary condition equations will be written with both of them present. The two other boundary conditions on the system concern the condition of the electron beam as it enters the system. For the present purposes

the beam will be considered unmodulated on entrance, so that the a.c. beam current and its first derivative will be set equal to zero. These four boundary conditions are stated mathematically in Eqs. 19 through 22. First, the circuit current at the left can be found from Fig. 1, Eq. 2 and Eq. 3, modified for the end section

$$I_a - V(0)Y_a = jV(0)\left[Y_o(\cot\theta_o - e^{j\theta}\csc\theta_o) + j\frac{Y}{2}\right] \tag{16}$$

$$= jV(0)\,Y_o\left[\cos\theta_1 - e^{j\theta}\right]\csc\theta_o \tag{17}$$

$$= jV(0)\,Y_o\left[\cos\theta_1 - \cos\theta - j\sin\theta\right]\csc\theta_o \tag{18}$$

The voltage $V(0)$ is the sum of voltages of four waves V_1 through V_4, corresponding to the characteristic roots x_1 through x_4 of Eq. 15, or four values of θ ; θ_1 through θ_4. Using the four amplitudes V_i, this boundary condition may be written

$$\sum_{i=1}^{4}\left[(Y_a + Y_o\frac{\sin\theta_1}{\sin\theta_o}) + jY_o\frac{\cos\theta_1 - \cos\theta_i}{\sin\theta_o}\right]V_i = I_a \tag{19}$$

At the other end, Eq. 1 is of use, but now the voltage $V(z) = \sum e^{-j\theta_i M} V_i$, where M is the total number of sections. The resulting equation is

$$\sum_{i=1}^{4}\left[(Y_b - Y_o\frac{\sin\theta_1}{\sin\theta_o}) - jY_o\frac{\cos\theta_1 - \cos\theta_i}{\sin\theta_o}\right]e^{-jM\theta_i}V_i = I_b \tag{20}$$

The beam current is the sum of partial waves also, and can be found directly from Eq. 6.

$$i_1(0) = -j\,2Y_o \csc\theta_o \sum_{i=1}^{4} (\cos\theta_1 - \cos\theta_i)\, V_i \qquad (21)$$

The derivative $\left.\frac{\partial i_1}{\partial z}\right|_{z=0}$ must also be zero. Since z variation is as $e^{-j\theta_i \frac{z}{\mathcal{L}}}$, this requirement becomes

$$i_1'(0) = -Y_o \csc\theta_o \sum_{i=1}^{4} \frac{\theta_i}{\mathcal{L}} (\cos\theta_1 - \cos\theta_i)\, V_i \qquad (22)$$

In considering the behavior near a stop band, the normalizations given in Eqs. 9 through 12 will be used, and all higher order terms in F will be dropped. It is convenient also to write the terminating impedances and current sources in normalized forms, using the following definitions:

$$Fb_a = (Y_a/Y_o)\sin\theta_o \qquad Fb_b = (Y_b/Y_o)\sin\theta_o \qquad (23)$$

$$FJ_a = (I_a/Y_o)\sin\theta_o \qquad FJ_b = (I_a/Y_o)\sin\theta_o \qquad (24)$$

The boundary condition equations are then given approximately by Eqs. 25 through 28

$$\sum_{i=1}^{4} (b_a - x_i)\, V_i = J_a \qquad (25)$$

$$\sum_{i=1}^{4} (b_b + x_i) e^{-jFMx_i} V_i = J_b \qquad (26)$$

$$\sum_{i=1}^{4} (x_1^2 - b_1^2)\, V_i = 0 \qquad (27)$$

$$\sum_{i=1}^{4} x_i(x_i^2 - b_1^2)V_i = 0 \qquad (28)$$

The x_i are the four roots of Eq. 15.

At this point there are several choices. This set of equations is capable of giving forward gain, backward gain, or the start oscillation condition, depending on the driving current used. In the present problem, attention was focussed on the condition for start oscillation initially in the range where the oscillation is of the backward wave type, and passing through the stop band into the range where oscillation, if any, is due to forward wave interaction. In between these regions, there can be a range of oscillations which are not clearly either forward or backward wave, and the transition between the two is continuous. This has been pointed out for a particular case by Gould[2].

Since we are principally concerned with the start oscillation condition, let us set both current sources equal to zero, giving a homogeneous set of equations. Then to find start oscillation conditions, the determinant of coefficients must be set equal to zero. Since this determinant is a complex number, it must be considered a function of two real variables in order to find its zero. The procedure used was to fix all variables except FM and b_e, and then determine the values of FM and b_e required for the determinant to become zero. The numerical results are given in Section III.

Comparison with conventional three-wave theory. To compare this approach with the conventional traveling-wave tube theory first developed by Pierce[4], we shall return to the exact characteristic equation, (8). Let us assume that $\theta_e \approx \theta_1 \neq \pi$ so the beam is

approximately synchronized with a forward wave, and the backward wave is definitely asynchronous. The first factor on the left of Eq. 8 can then be rewritten as a product.

$$\cos\theta - \cos\theta_1 = 2 \sin \frac{\theta + \theta_1}{2} \sin \frac{\theta_1 - \theta}{2} \tag{29}$$

To make this look like the Pierce theory, assume that $\theta \approx \theta_1$, and denote small differences by the relations

$$\theta_1 - \theta_e = \theta_e C b \tag{30}$$

$$\theta - \theta_e = -j \theta_e C\delta \tag{31}$$

Then (8) becomes approximately

$$\theta_e^3 C(b + j\delta) \sin\theta_1 \left[-C^2\delta^2 - \frac{\theta_q^2}{\theta_e^2} \right] = - \frac{I_o}{4Y_o V_o} \sin\theta_o \theta_e \tag{32}$$

in which it is assumed $\theta_q \ll 1$. If we now set $\theta_q^2/\theta_e^2 = 4QC^3$, and

$$C^3 = \frac{I_o}{4Y_o V_o} \theta_e^2 \frac{\sin\theta_o}{\sin\theta_1} \frac{\sin\theta_q}{\theta_q} \tag{33}$$

we are left with Pierce's determinantal equation for more conventional traveling wave tube analyses.

$$(\delta^2 + 4QC)(b + j\delta) = -1 \tag{34}$$

If the Pierce impedance, $E^2/2\beta^2 P$ is calculated for the circuit model used, and used in the expression for C^3, the result is the same except that θ_1^2 replaces θ_e^2. This is, of course, consistent with the assumptions usually used in the Pierce theory.

The comparison of boundary conditions is somewhat more difficult, but it is not hard to see that the system of Eqs. 19 through 22 reduces to three equations if $\theta_1 \approx \theta_e \approx \theta\pi$. To see this, examine these as they might appear in finding the gain of a traveling wave tube. For three of the roots, $\theta_1 \approx \theta_1$ but for the fourth $\theta_i \approx -\theta_1$. Taking this root to be θ_4, we note that this represents the backward traveling wave, and its amplitude may be reduced to zero approximately by adjusting the terminating admittance Y_b, so that

$$Y_b = Y_o \frac{\sin \theta_1}{\sin \theta_o} \tag{35}$$

In this case, the $i = 1$, 2, and 3 terms of (20) are small, while the fourth one is large, since $\sin \theta_4 \approx -\sin \theta_1$. Thus, Eq. 20 says approximately

$$V_4 = 2I_b e^{jM\theta_4} \frac{\sin \theta_o}{Y_o \sin \theta_1} \tag{36}$$

If $I_b = 0$, only the first three voltage amplitudes enter into the boundary conditions. In this manner the assumption usual in this type of analysis has been made explicit. That is, the collector end of the tube is matched and thus there is no reflected wave.

The remaining Eqs. 19, 20, and 21, each with $V_4 = 0$, can be adjusted to give the familiar equations for traveling-wave tube gain as customarily used. To do this, one must use the small C approximations and expansions as done in the discussion above of the determinantal equation.

Table I gives a summary of the relationships among the present

quantities and those customarily found in traveling-wave tube analysis. The approximate equalities hold far from a stop band ($b_1^2 >> 1$) .

TABLE I

$$j\delta = \frac{F}{\theta_e C}(x - b_e)$$

$$b + jd = \frac{F}{\theta_e C}(b_1 - b_e)$$

$$F^4 \approx \left|2 \sin \theta_1\right| \theta_e^3 C^3$$

$$F \approx (2b_1)^{1/3} \theta_e C$$

$$FM \approx (2b_1)^{1/3} 2\pi CN$$

$$(FM)^4 = 2M \sin \theta_1 (2\pi CN)^3$$

Space-charge parameters. In the accompanying computations, a space charge parameter b_q has been used because of the simple form which this gives to the determinantal equation. In this respect it is similar to QC in the three-wave analysis. Note that QC varies both with beam current and voltage. It is Q (and also Q/N) which is a function of geometry. Johnson[5] has used Q/N at start oscillation as a convenient geometrical parameter which can be written as QC/CN . Both of these latter quantities can be found from the generalized analysis.

In an analogous way, one should find the dependence of b_q^2 on current and voltage, and find a space charge parameter which is a

function only of geometry. Consider first the defining relation for b_q

$$F^2 b_q^2 = \theta_q^2 = \frac{\omega_q^2}{\omega^2}\theta_e^2$$

or, near the band edge,

$$F^2 b_q^2 \approx \theta_e^2 \frac{\omega_q^2}{\omega^2} = \frac{\pi I_o \theta_e^2 R}{\omega^2 \epsilon_o m (2\eta V_o)^{3/2}}$$

The current dependence of this function can be removed by a division by F^4. That is, b_q^2/F^2 is independent of current. This quantity will be given a specific name, $Q_1^2 = b_q^2/F^2$ and thus the parameter Q_1/M, is a function of geometry and is constant for a given tube and frequency regardless of current. This quantity Q_1/M at start oscillation is plotted where necessary in the section concerning numerical results.

Application of the analysis to the helix. The helix as a slow wave circuit poses some special problems in this analysis because of its skew symmetry. As a result of this symmetry, the field patterns for the fundamental and the first backward space harmonic in the absence of a stop band are different. The former vary with radius as the modified Bessel function of zero order, I_o, while the latter vary as the corresponding function of first order, I_1. In the presence of periodic loading, and thus a stop band, these field patterns will no longer be correct, and near the band edge the field patterns will be thoroughly mixed between the two modes. Thus in the

immediate vicinity of a band edge, the theory should be applicable when applied to a filamentary beam at some location in the helix. The closer the beam is to the surface of the helix itself, the better the theory will hold over an average of phase shift, since the impedances measured right at the surface of the helix are functions principally of the phase shift and wire configuration, and are the same for either wave at a specified phase shift.

To consider the physically useful case, where the beam is not filamentary, one must use in the impedance calculation, the mean square value of electric field averaged over the area of the beam. Again, the theory is difficult to apply exactly in many cases due to the different interaction impedances presented by the two waves. For a thin hollow beam near the surface of the helix, the two impedances are very nearly equal, and this theory may be directly applied. For a solid beam on the axis of a helix, the coupling to the backward wave is weaker than that to the forward wave. It seems that one should use some sort of weighted average impedance, but the exact nature of the weighting function has not been ascertained.

If the stop band is very small, as that due to a small perturbation on the helix, the present theory cannot be applied to any useful result due to the different space patterns of the two waves, and the relatively important effect of small values of $\sin \theta_o$ which will then appear in the equations.

As a result of the above restrictions, when a helix is considered the present theory can only be applied where the stop band is

large enough that $Fb_1 \ll \sin \theta_o$ near the band edge. Furthermore, the number to be used for interaction impedance should be some sort of average of the impedances of the forward space harmonic and the backward space harmonic. Fortunately, the coupling parameter, F , is only proportional to the fourth root of this impedance, and the result is correspondingly insensitive to the exact weighting function. It seems reasonable to use the geometrical mean of these impedances near the band edge, while realizing that sufficiently far in either direction the impedance must be just that of the uncoupled wave.

Fortunately, this difficulty does not exist in any circuit for which the stop band is an intrinsic property of the circuit and not a perturbation. Such circuits as the folded waveguide, disc-loaded waveguide, cloverleaf, or other coupled cavity circuits, have the same spatial form in both space harmonics and thus can be discussed with no ambiguity in the coupling impedance which appears in the normalizing quantity F .

Comparison with Gould's analysis. Since this paper has drawn from time to time upon a previously published paper by Gould[2], who discussed a coupled cavity circuit in a similar context, it is worth while at this point to make a short comparison between the two analyses. To do this, we turn immediately to the circuit model (Fig. 3) and characteristic equation, (37), used by Gould. The characteristic equation used in this paper is written below it for convenience. The left side of Gould's equation has been written to

coincide with Eq. 38 of the present paper, and the two right sides are to be compared. Up to this point, there have been no approximations beyond those assumed in the circuit models.

$$(\cos\theta - \cos\theta_1)\left[4\sin^2\frac{(\theta-\theta_e)}{2} - 2(1-\cos\theta_q)\right] \tag{37}$$
$$= \frac{I_o}{4V_o}\sqrt{\frac{\mathcal{L}}{C}}\ \frac{\lambda}{k}\theta_e\ \frac{\sin\theta_q}{\theta_q}(1+2k\cos\theta_1)(1+2k\cos\theta)$$

$$(\cos\theta - \cos\theta_1)\left[4\sin^2\frac{(\theta-\theta_e)}{2} - 2(1-\cos\theta_q)\right] \tag{38}$$
$$= \frac{I_o}{4V_o}Z_o\sin\theta_o\theta_e\ \frac{\sin\theta_q}{\theta_q} = 2F^4$$

To compare these, one should also introduce the conventional coupling impedance of each circuit. In Gould's analysis

$$K = \frac{\sqrt{\mathcal{L}/C}}{\lambda^3 k\,\theta^2\sin\theta} \tag{39}$$

and in the present paper:

$$K = \frac{Z_o\sin\theta_o}{\theta^2\sin\theta_1} \tag{40}$$

With these interaction impedances set equal to each other, the comparison between these two approaches reduces to the following approximate equality, after cancelling common factors:

$$(1+2k\cos\theta_1)(1+2k\cos\theta)\,\lambda^4 \approx 1 \tag{41}$$

That this is indeed an equality to within the approximation $\theta \approx \theta_1$ results from Gould's equation for θ_1, which is (for lossless circuits)

$$1 + 2k \cos \theta_1 = \frac{1}{\lambda^2} \tag{42}$$

Thus these two circuit models give identical characteristic waves within a very good approximation, based only on the use of generalized circuit quantities, phase shift per section, and interaction impedance. If these quentities can be calculated or measured (and of course impedance will become infinite at the band edge), the behavior of the traveling-wave tube near the band edge can be calculated from the accompanying theory regardless of the most appropriate exact circuit model. It should be noted that the application of the theory to circularly symmetric circuits such as the coupled cavity type does not result in complications such as arose in the case of the helix.

3. Numerical Results

In order to apply the theory developed to the problem of backward wave oscillation near a band edge, it is necessary to solve Eqs. 25 through 28. The condition of incipient oscillation occurs when the determinant of coefficients of this system of equations equals zero. It is this condition which was coded for the Datatron 205 computer and solved for the cases presented here. The numerical procedure is the following. First the machine solves the quartic equation for the characteristic roots (Eq. 15). These roots are then

substituted in Eqs. 25-28 and the determinant evaluated. If the determinant is smaller than a pre-assigned tolerance, the assumed quantities are considered to be solutions. If the determinant is larger than the tolerance, a two-dimensional form of Newton's method is used to find a second approximation to the independent variables. Any two of the quantities b_e , b_l , b_q , FM , b_a , or b_b might be used as independent variables. In practice it is found that FM and b_l are most convenient, although FM and b_e were used for a few cases. In general, the approximation method is repeated until the results satisfy the tolerance or until the search is arbitrarily stopped as being fruitless.

In order to usefully tabulate the results, they must be reconverted to parameters more closely related to physical operation than those appearing in the determinant. To do this, we note that the quantity FMb_e is the amount by which the total phase shift on the (uncoupled) beam would deviate from πM . Similarly, the quantity FMb_l is the amount by which the circuit phase shift would differ from πM in the absence of the beam. The quantities Fb_a and Fb_b are normalized admittances appearing at either end of the tube. The numerical output will be plotted as much as possible in terms of those quantities.

Typical results of the numerical calculations are shown in Figs. 4 and 5. The solid curve represents FM and the dashed curve FMb_l at start oscillation for the parameters stated. From these curves a number of interesting things can be noted. First, if the

terminal admittances represent perfect cold circuit terminations at all frequencies, the correct terminal conditions are $b_a = b_b = b_1$. As shown in Fig. 4 this results in a zero value of start oscillation current at exactly $b_1 = 0$, that is, at the band edge.

As a matter of fact, the curve of Fig. 4 corresponds exactly to CN = .314. In other words, if the circuit is perfectly matched in the absence of a beam, the three-wave theory predicts the starting conditions exactly. Of course, as the band edge is approached, matching becomes more and more difficult. It is expected that finite circuit loss would have a major effect on curves such as Fig. 4, removing the sharp dip to FM = 0 .

Fig. 5 shows a typical result when b_a and b_b are held constant as the beam voltage (b_e) is varied. The start oscillation current (represented by the parameter FM) is seen to go through a broad minimum at a beam velocity slightly higher than that required for synchronism at the band edge. Note, however, that the frequency of oscillation represented by b_1 does not actually reach the band edge until a somewhat higher voltage is reached. Thus the lowest start oscillation current does not produce oscillation at the band edge, but rather at a slightly lower frequency.

This figure illustrates the behavior of the higher order modes, and also the transition between backward wave oscillation (on the right hand part of the picture, where b_e is positive), and forward wave oscillation engendered by reflections from the mismatched terminations (left side of the figure where b_e is negative). It is

seen here that the oscillation conditions transform smoothly from backward wave to forward wave, and that the various modes of forward wave oscillation appear to come in one at a time from the higher current forms of backward wave oscillation in the course of the transition. One can see on the left side of this figure, the typical pattern followed in forward wave feedback oscillators in which the frequency changes discontinuously at some voltage because the curves of the threshold current (FM) cross each other. Although the present theory loses accuracy as one goes far from the stop band, it is interesting to see that it predicts the well-known behavior in this region.

In the course of the computations, many curves of the general nature illustrated in Figs. 4 and 5 were calculated and plotted. These were the most convenient formulations mathematically, but other curves are likely to be of more use practically. In Figs. 6, 7, and 8, the minimum values of FM for start oscillation have been plotted as a function of the terminating admittances for three cases of space charge parameter b_q. It is seen that the minimum start oscillation current rises steeply as a function of terminating admittance up to a maximum near $FMb_a \approx 2.5$, and then drops off slowly with further increase of the admittance. The general form is independent of space charge although the numbers are slightly different. A number of cases have also been calculated where b_a and b_b are not equal, and some for which they are complex. In all of these cases which have been calculated so far, the maximum of the curves

equivalent to Fig. 5 through 8 falls below but near to the values for equal, resistive terminations. At present there is no fundamental mathematical or physical explanation for this fact, and the extra degrees of freedom in assigning initial parameters have precluded a systematic numerical study.

Having obtained curves of the form of Figs. 6 through 8, it appears that for optimum suppression of oscillations at the band edge, one should pick the value of terminating admittance which gives the maximum. Having done this, we recognize that the admittances are not constant with frequency in these figures since the parameters b_a and b_b have been fixed in such a calculation. By cross plotting from the curves available, we have obtained the curves shown in Figs. 9 through 11, which predict the start oscillation current as a function of frequency for fixed terminating impedances which were first selected from the maxima of Figs. 5 through 7.

4. Interpretation

Having achieved a considerable mass of numerical data, we should now ask in what way this data can be applied to traveling wave tube design. There are two cases in which stop bands may be used for the suppression of backward wave oscillation. In one case, typified by the helix, a tube is to be operated continuously, but there is a backward wave which can cause oscillations. A stop band may be inserted in such a location that the electron beam is

no longer synchronous with any backward wave component. The present theory is capable of giving an estimate of the width which may be required in this stop band. A second possible case is that in which a tube is operated on a pulsed basis, and oscillations can occur as the voltage is rising and falling, although they will not be in synchronism during the flat topped part of the pulse. Such oscillations have been given the name "rabbit-ears" because of the characteristic pips which they add to the detected output pulse. While the present theory is applicable to this type of oscillation, it appears to indicate that they cannot be eliminated with a lossless circuit and any reasonable values of interaction. The details of the interpretation follow.

a) Oscillation suppression by stop bands. In this case, we shall assume that the interest is concentrated on the output section of a high power traveling wave tube for continuous operation. A stop band has been created so the mathematical analysis of the earlier sections is approximately valid. We expect that the termination on the input end will be some sort of tapered attenuator which ought to be a fairly good match up to frequencies fairly close to the stop band. On the other end, the termination is the output connector, which is presumably matched over the operating band, and is thus probably about equal in impedance to the midband characteristic impedance of the slow wave circuit. The paper published by Siegman and Johnson[3] gives a discussion of this mode of operation, and Fig. 12 shows the comparison between the present theory and the published curve in that paper. To generate this comparison it was

assumed that the knee of the curve of start oscillation current versus voltage (Siegman and Johnson, Fig. 19) occurs at $\theta_1 \approx \pi$. Then the curve is traced back to the point where the classical theory is assumed to hold. At that point (I_o = 1 ma, V_o = 1300 v. in the present case), CN, QC, and θ_1 are found from conventional theories[5,6] and FM from

$$(FM)_p^4 = 2M \sin \theta_1 (2\pi\, CN)^3 \tag{43}$$

FM in the stop band is then

$$(FM)_s^4 = (FM)_p^4 \frac{\sin \theta_{os}}{\sin \theta_{1p}} \tag{44}$$

The subscript s signifies stop band and p signifies the pass band. It is assumed that in the pass band region $\theta_1 = \theta_o$, and that θ_o is linearly proportional to frequency, equaling π in the center of the stop band.

b) The suppression of "rabbit ears" oscillation in pulsed tubes.

In order to suppress this type of transient oscillation, we would need a circuit whose start oscillation current never is lower than the value which the tube will have as the voltage swings through the backward wave frequency range. Unfortunately, one can determine fairly quickly from the curves of this paper that the current will always exceed the start oscillation current by an appreciable factor if high gain is desired in the output section. Assume a tube with gain maximum at $\theta_o = \pi/2$ and assume that CN = .5 or more is required in the output section. We use subscripts o for forward wave operation and 1 for the backward wave oscillation.

$$C_o N_o = .5 \tag{45}$$

$$M = 4N_o \tag{46}$$

$$(FM)^4 = (2\pi\, CN)^3 M \sin \theta_1 \tag{47}$$

$$(F_o M_o)^4 = 31\, M \tag{48}$$

For wide stop bands (k small, or $\theta_o \approx \frac{\pi}{2}$)

$$(F_1 M_1)^4 \approx (F_o M_o)^4 \frac{I_{01} V_{00}}{V_{01} I_{00}} \tag{49}$$

If perveance is constant, this becomes

$$F_1 M_1 \approx F_o M_o \left(\frac{V_{01}}{V_{00}}\right)^{1/8} \tag{50}$$

and the latter factor is very near unity. Thus

$$F_1 M_1 \approx 2.36 \sqrt[4]{M} \tag{51}$$

Even if $C = 0.2$, $N = 2.5$, $M = 10$, and $F_1 M_1 = 4.2$. (52)

From Figs. ~~3c~~ 9 through ~~3e~~ 11 it appears that this tube will exhibit "rabbit-ears" oscillations. Note that the situation worsens as M increases, making high-C tubes preferable to those with lower C, at least in this respect.

ACKNOWLEDGMENT

The bulk of the numerical work for this project was done by Mr. R. E. Tokheim, whose help is gratefully acknowledged.

REFERENCES

1. Reutz, J. A. "Microwave Interaction of Electron Beams and Non-Propagating Periodic Structures", Stanford Electronics Laboratories, Tech. Report No. 30, (Project 204), March 27, 1958.

2. Gould, R. W. "Characteristics of Traveling-Wave Tubes with Periodic Circuits", Transactions of the IRE, PGED, July 1958.

3. Siegman, A.E. and Johnson, H.R., "Suppression of Backward Wave Oscillation by Filter Helix Methods", Transactions of the IRE, PGED, April 1955.

4. Pierce, J. R. Traveling-Wave Tubes, D. Van Nostrand, 1950.

5. Johnson, H.R. "Backward Wave Oscillators", Proc. IRE, June 1955, page 684.

6. Weglein, R.D. "Backward Wave Oscillator Starting Conditions", Transactions of the IRE, PGED, ED-4, No. 2, page 177 (April 1957).

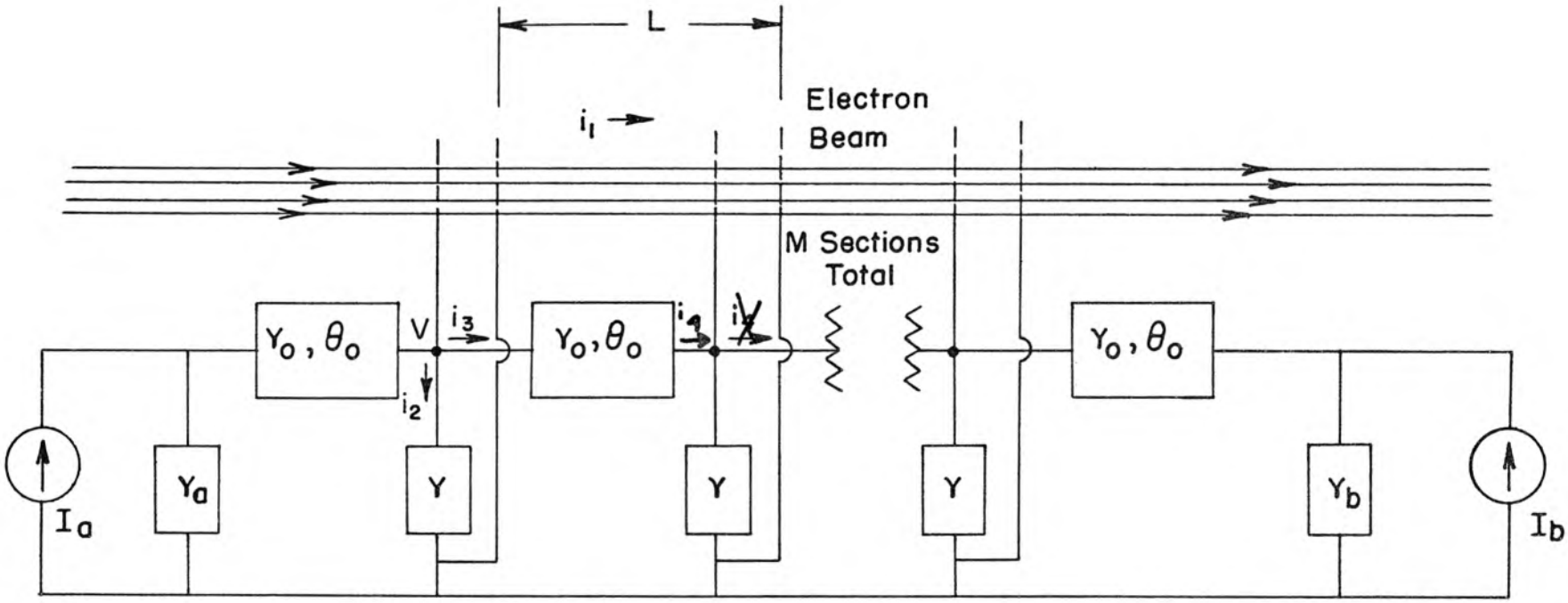

FIG. 1

Equivalent circuit used for the analysis, including arbitrary impedances and generators at each end of the circuit.

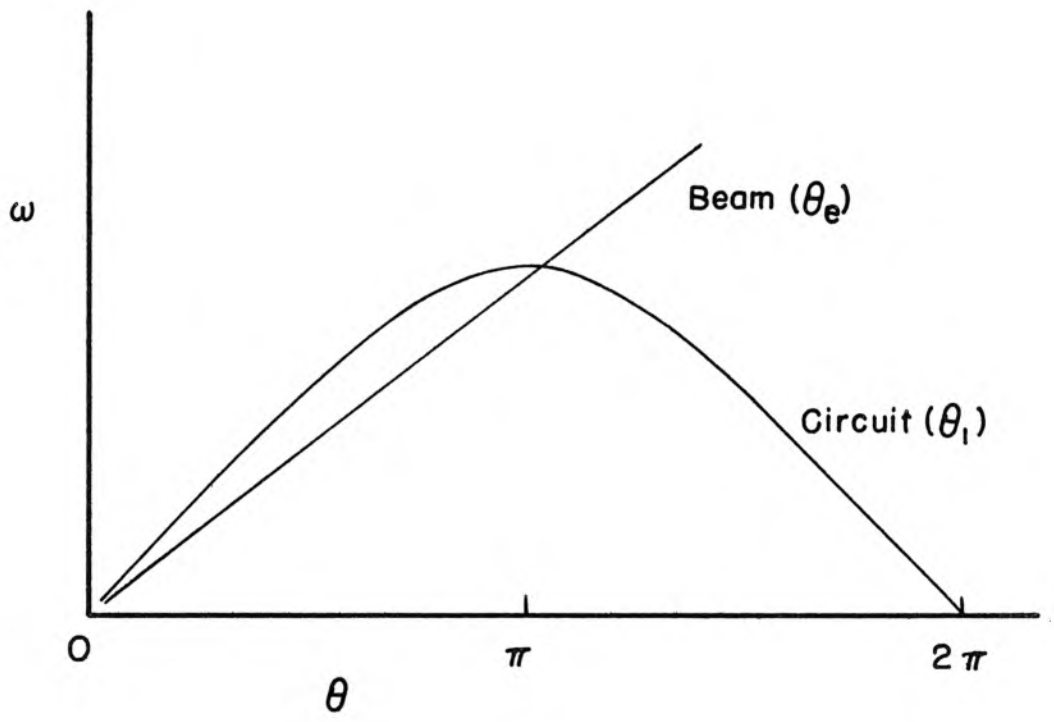

FIG. 2

Synchronism of an electron beam velocity with the cutoff frequency of a slow wave circuit.

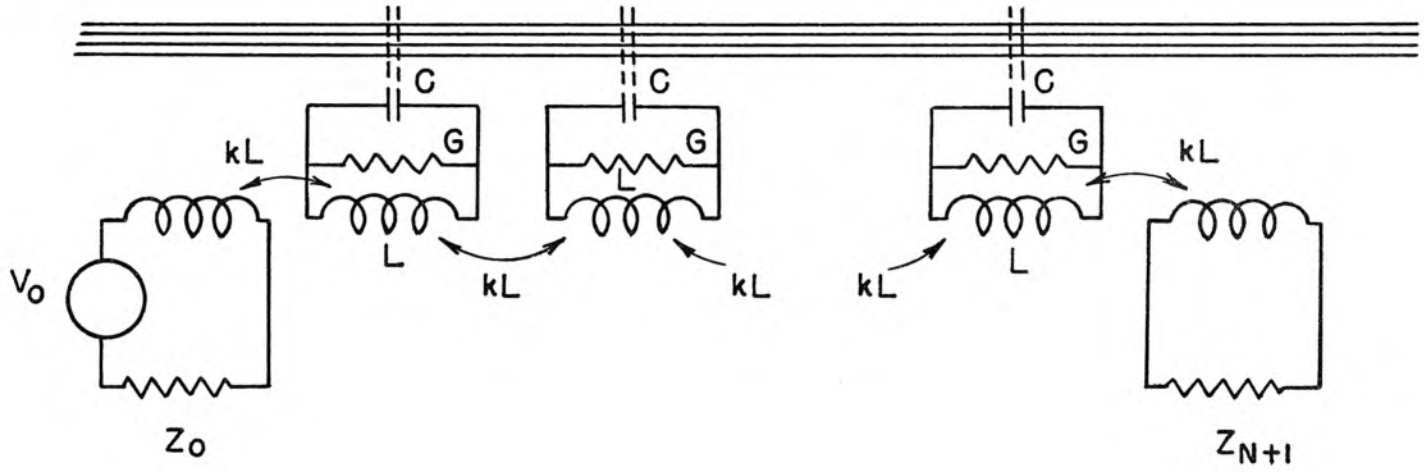

FIG. 3

Circuit model used by Gould in analyzing periodic traveling wave tubes. As long as k is small, this circuit is equivalent to the one used in this paper, with appropriately chosen values of Z_o and θ_o .

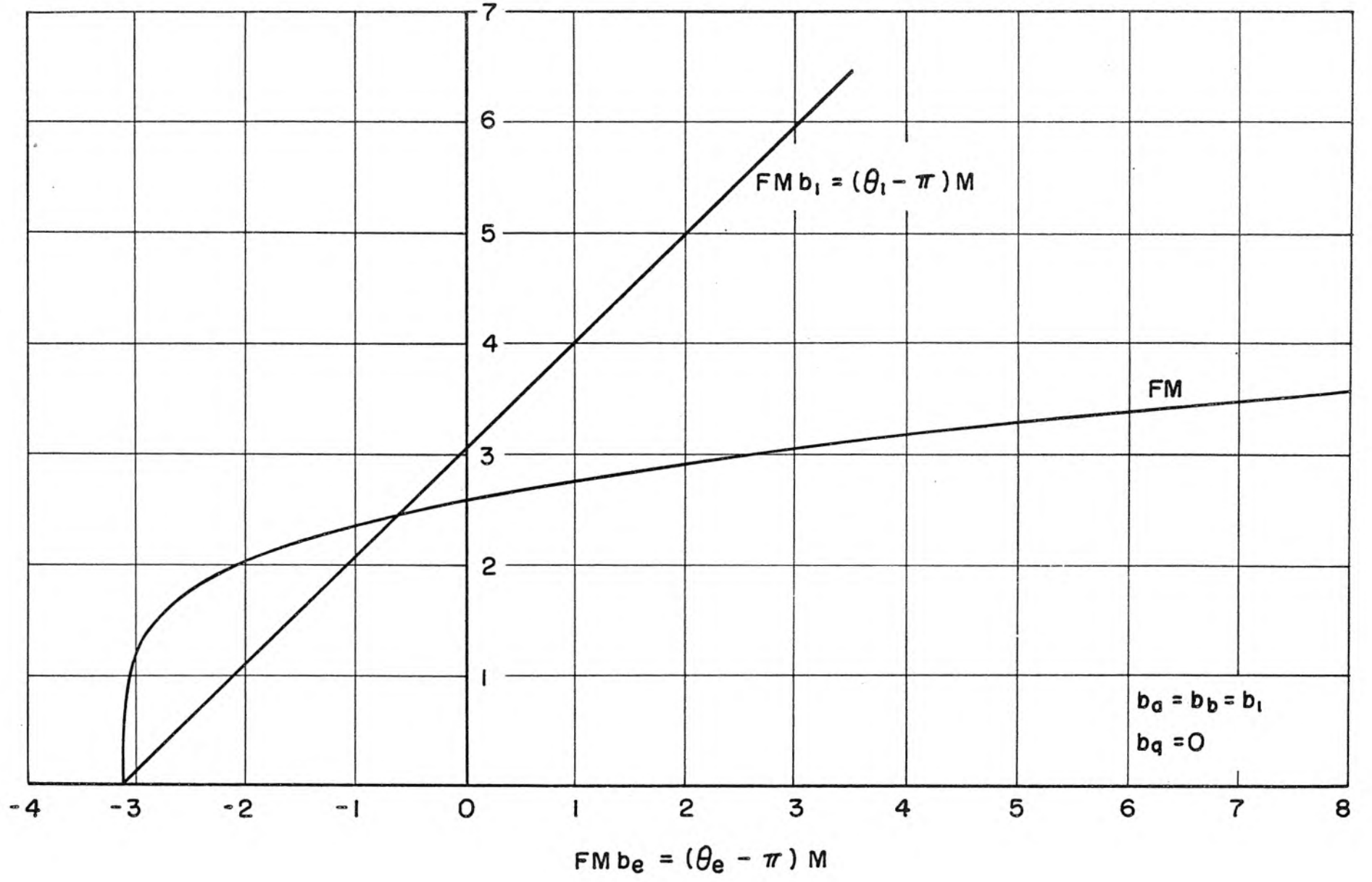

FIG. 4

FM at start oscillation versus beam phase shift for no space charge, when the terminations are perfectly matched at all frequencies. This curve is identical to that given by CN = .314, b = 1.52 .

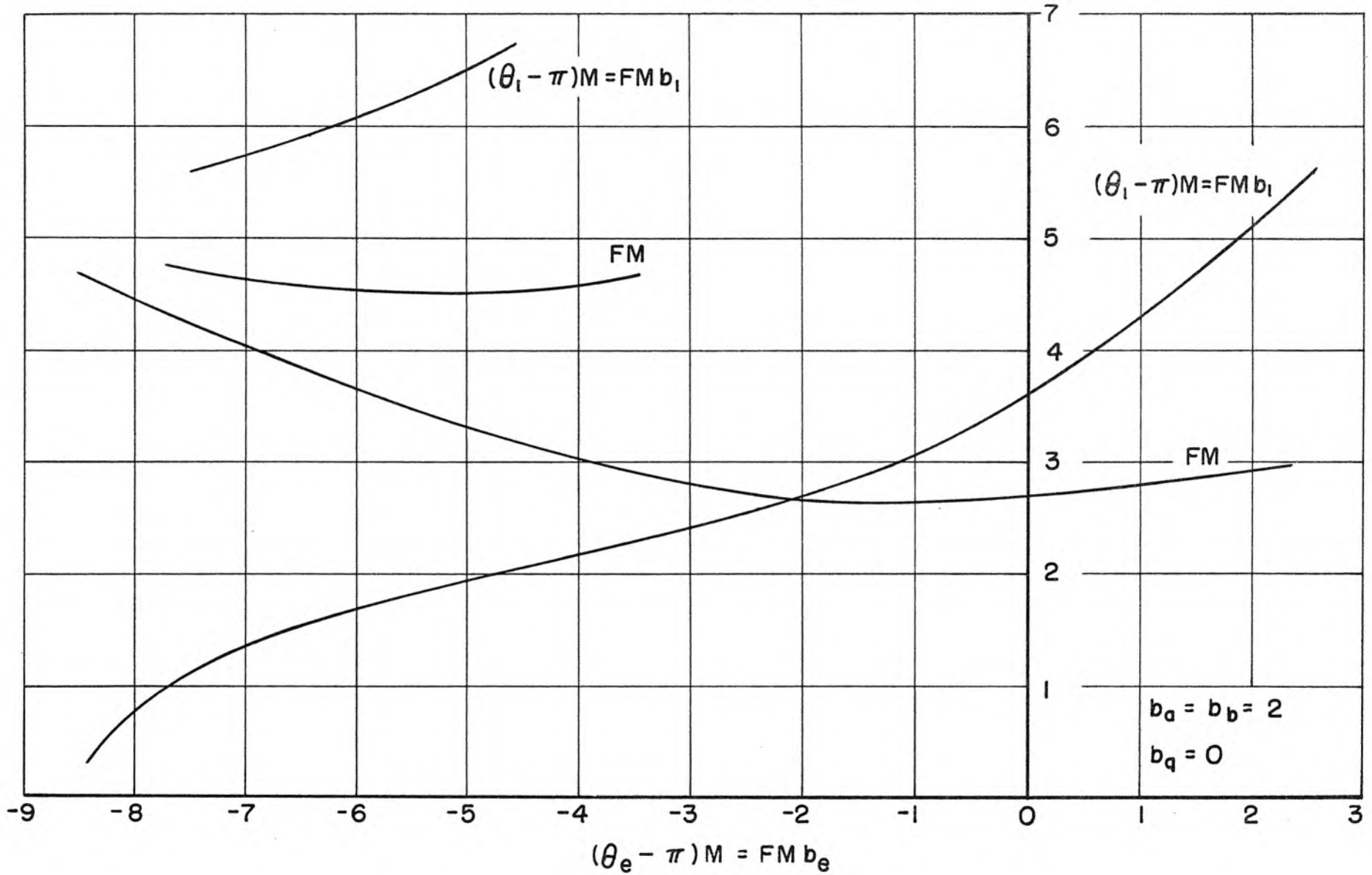

FIG. 5

FM at start oscillation versus beam phase shift for no space charge and finite terminations. This curve is expressed in terms of the basic equations, and thus corresponds to varying terminating admittances, FMb_a and FMb_b .

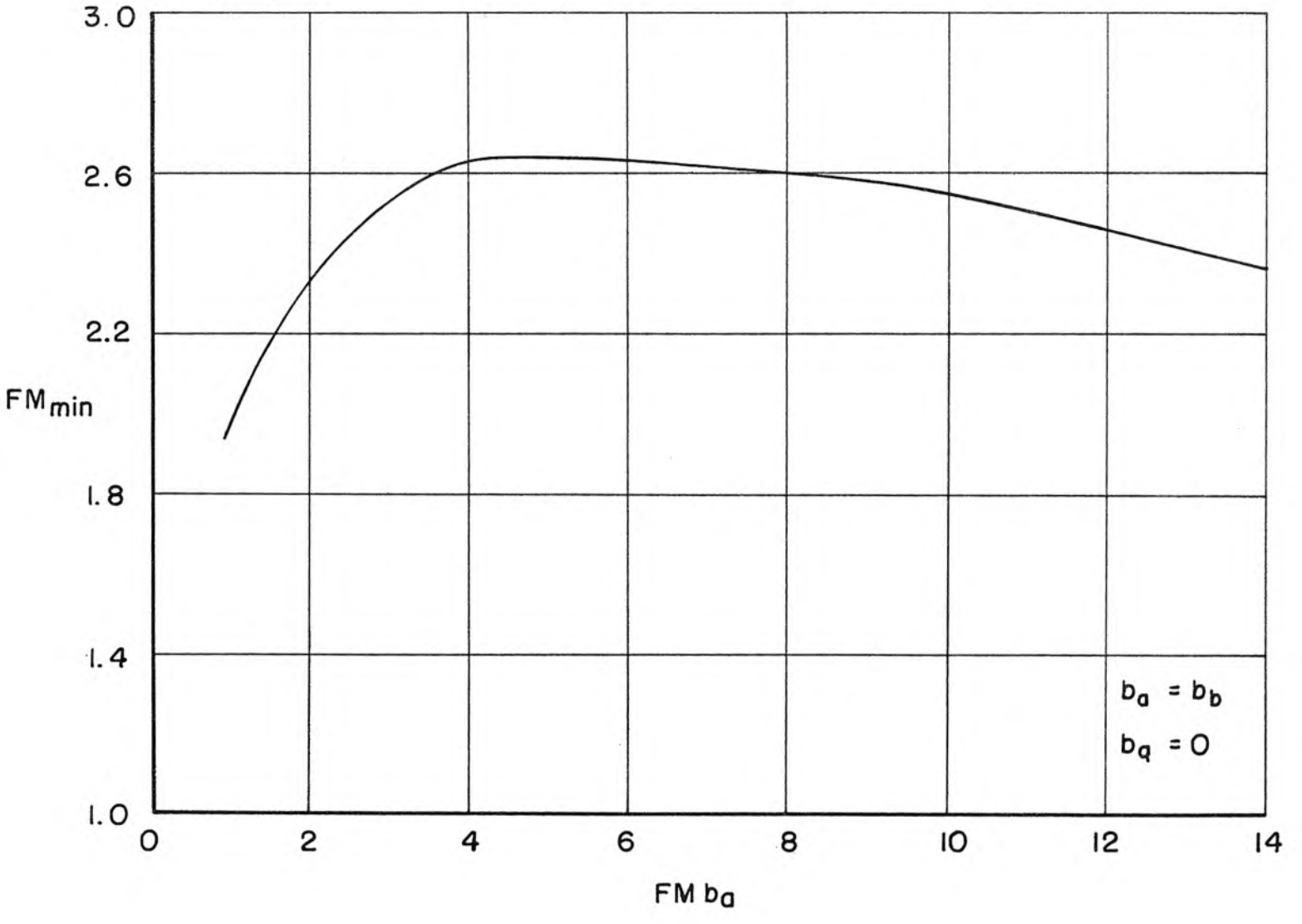

FIG. 6

Minimum value of FM (on curve such as Fig. 5) as a function of b_a ($b_b = b_a$), $b_q = 0$) .

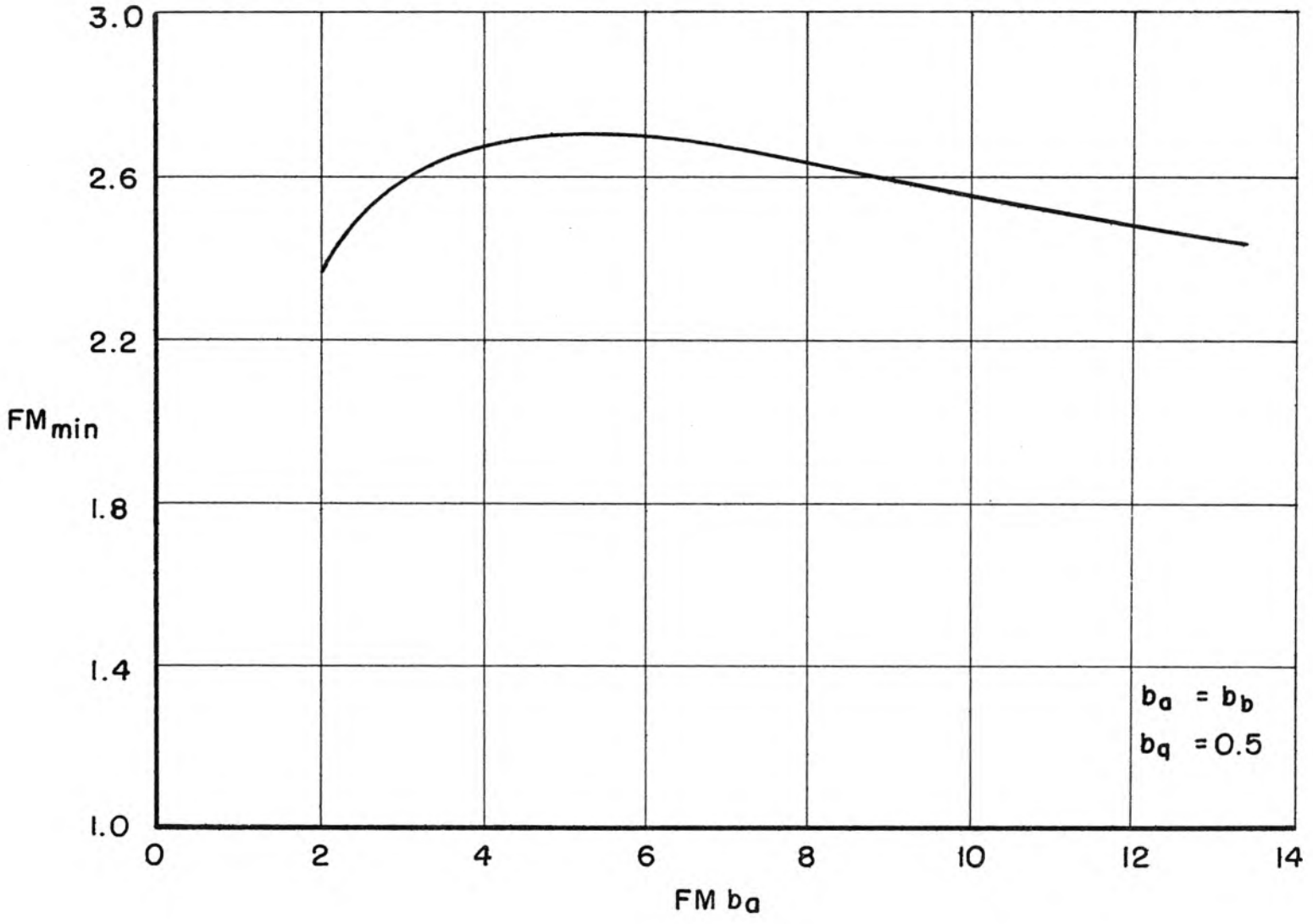

FIG. 7

Minimum value of FM (on curve such as Fig. 5) as a function of b_a ($b_b = b_a$), $b_q = 0.5$.

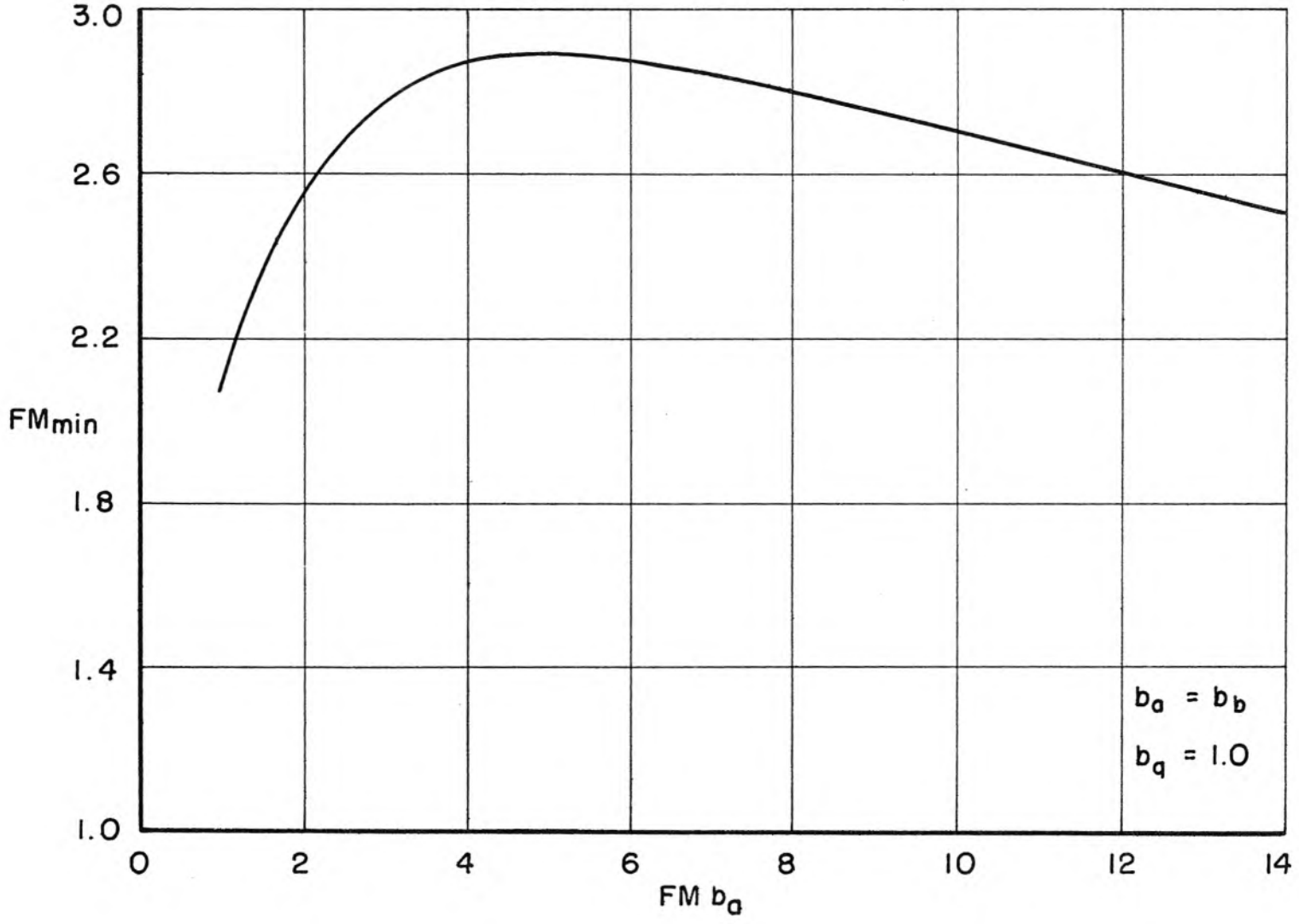

FIG. 8

8. Minimum value of FM (on curve such as Fig. 5) as a function of b_a ($b_b = b_a$), $b_q = 1.0$.

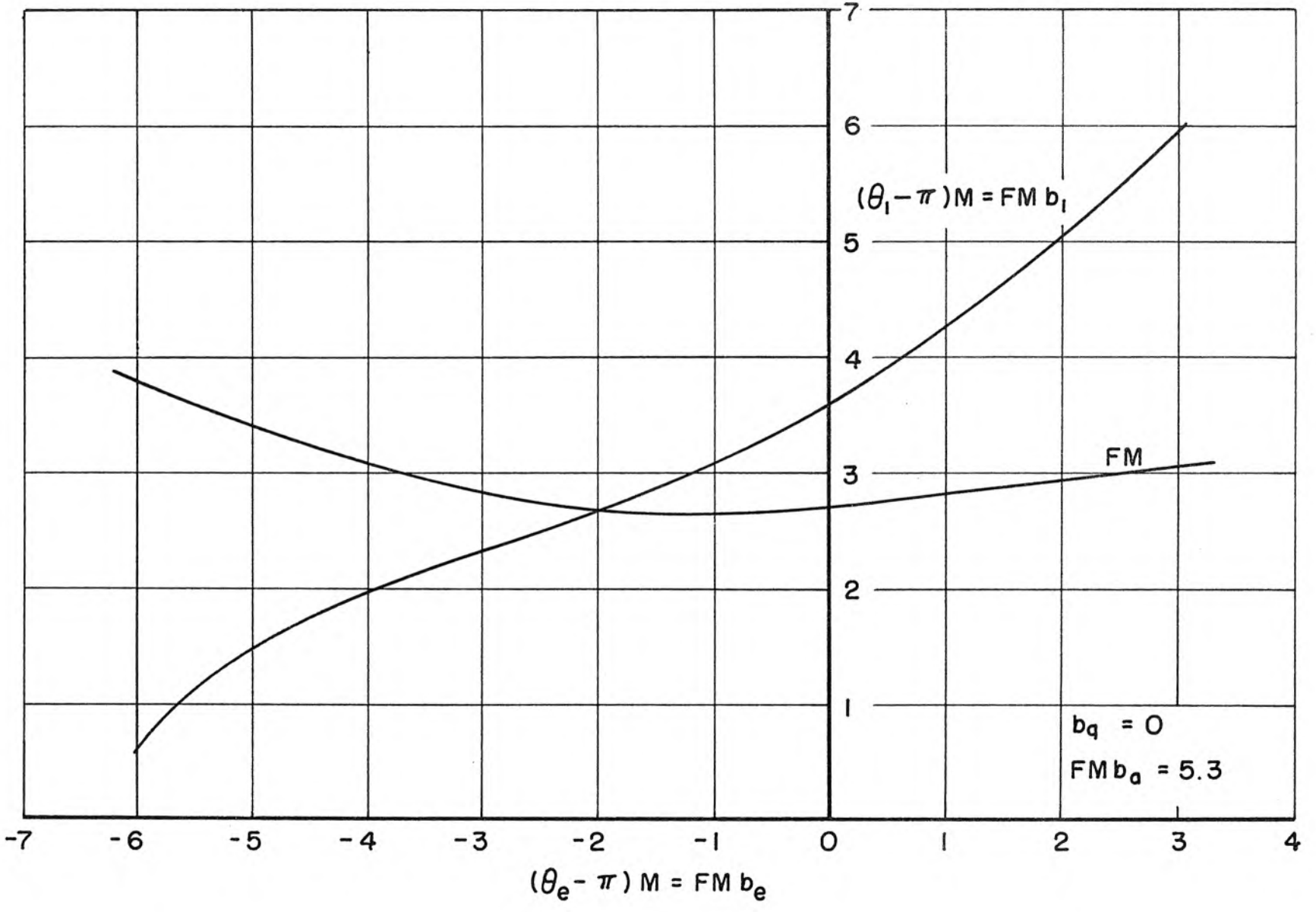

FIG. 9

FM at start oscillation versus beam phase shift with FMb_a and FMb_b chosen from the maximum of Fig. 6, $b_q = 0$. (Terminating admittances fixed for maximum oscillation.)

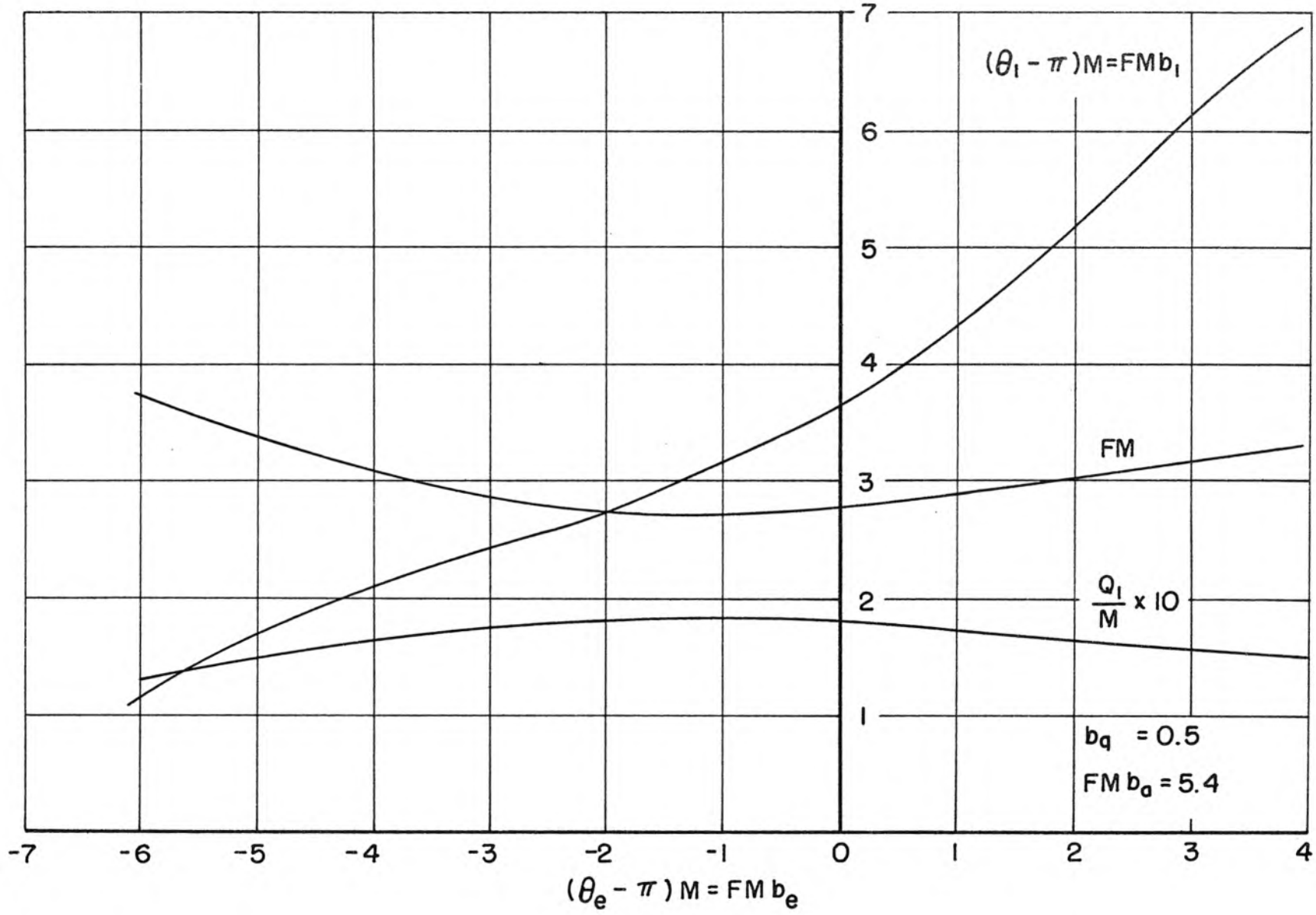

FIG. 10

FM at start oscillation versus beam phase shift with FMb_a and FMb_b chosen from the maximum of Fig. 7. $b_q = 0.5$. (Terminating admittances fixed for maximum oscillation suppression).

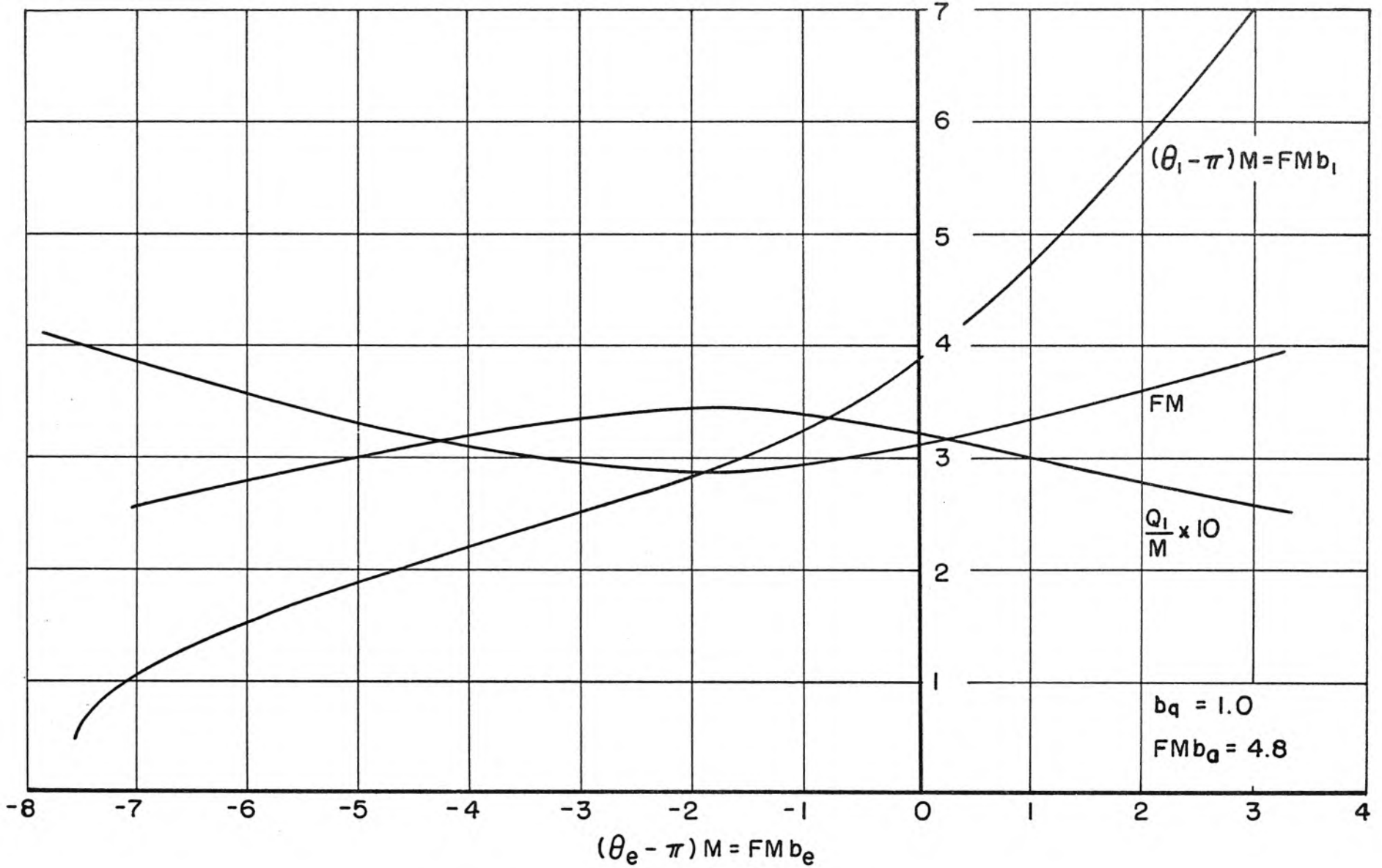

FIG. 11

FM at start oscillation versus beam phase shift with FMb_a and FMb_b chosen from the maximum of Fig. 8. $b_q = 1.0$. (Terminating admittances fixed for maximum oscillation suppression).

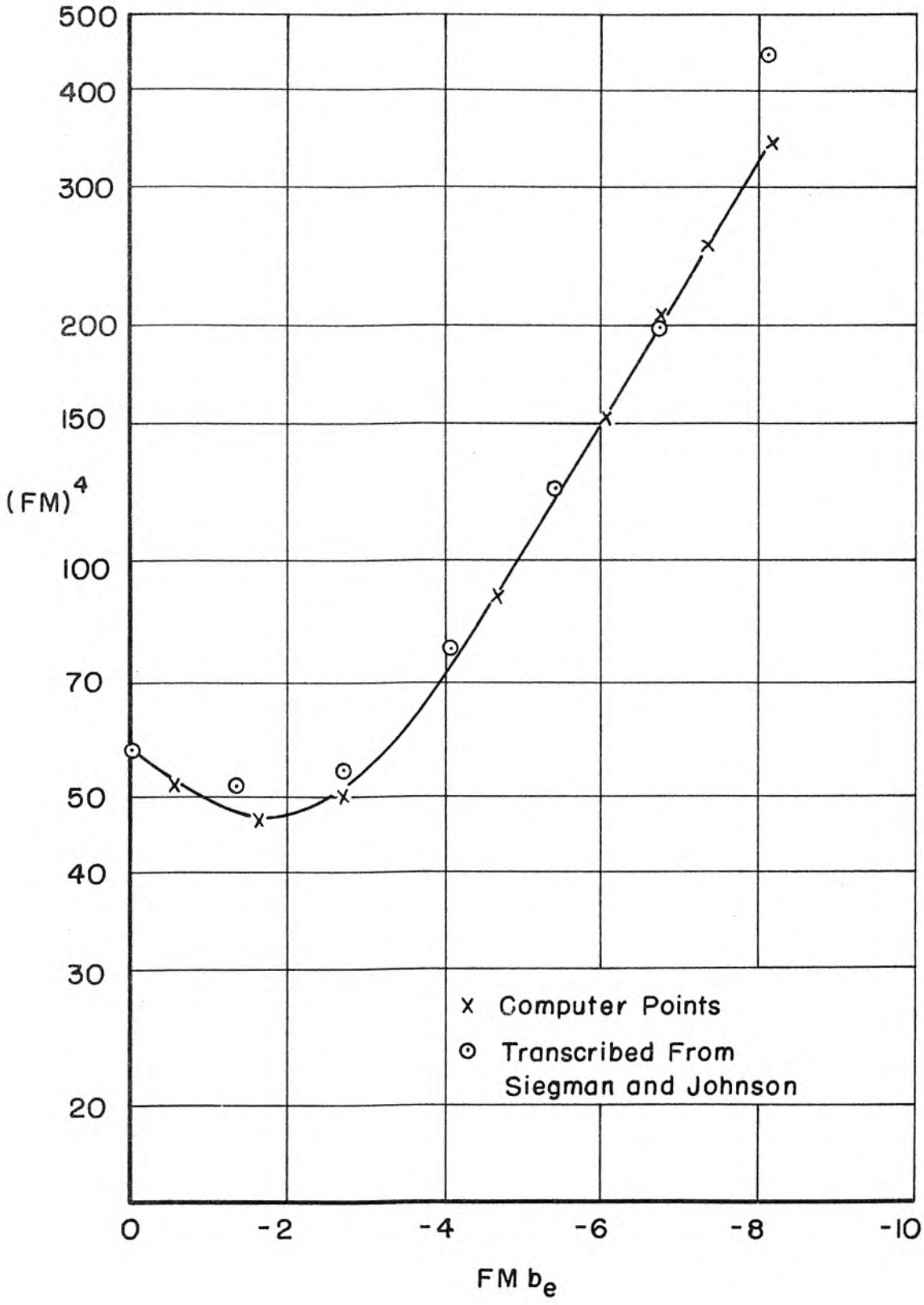

FIG. 12

Comparison of theory with published experimental results (Siegman and Johnson[3], data from their Figs. 18 and 19). The circled points were based on data taken from the published paper. The x's represent points computed by the present theory.

DISTRIBUTION LIST

Chief of Naval Research 2
Navy Department - CODE 427
Washington 25, D. C.

Director, Naval Research Lab.
Washington 25, D. C.
Attn: CODE 5240 1
CODE 7130 1
CODE 2000 6
CODE 5430 1

Commanding Officer 1
ONR Branch Office
1000 Geary Street
San Francisco, California

Scientific Liaison Officer 25
ONR, London
c/o Navy 100, Box 39, FPO
New York, New York

Commanding Officer 1
ONR Branch Office
1030 E. Green Street
Pasadena, California

Commanding Officer 1
ONR Branch Office
The John Crerar Library Bldg.
86 E. Randolph Street
Chicago, 1, Illinois

Commanding Officer 1
ONR Branch Office
346 Broadway
New york 13, New York

Officer-in-Charge 3
Office of Naval Research
Navy No. 100
Fleet Post Office
New York, New York

Chief, Bureau Aeronautics EL4 1
Navy Department EL43 1
Washington 25, D.C. EL45 1

Chief, Bureau of Ordnance
Navy Department Re 4 1
Washington 25, D. C. Re 9 1

Chief of Naval Operations Op 20X 1
Navy Department Op 421 1
Washington 25, D.C. Op 55 1

Director, Naval Ordnance Lab. 1
White Oak, Maryland

Director, Naval Electronics Lab 1
San Diego 52, California

Dept. of Electronics Physics 1
U.S.Naval Post Grad. School
Monterey, California

Commander Code 366 1
Naval Air Missile Test Center
Point Mugu, California

U.S. Naval Proving Ground 1
Attn: W. H. Benson
Dahlgren, Virginia

Commander 1
U.S.Naval Air Development Center
Johnsville, Pennsylvania

Committee on Electronics 1
Research and Development Board
Department of Defense
Washington 25, D. C.

Director, Natl. Bureau of Stds. 1
Washington 25, D. C.
Attn: Div.14.0 CRPL, Librarian

Commanding Officer 1
Engineering Res.and Dev. Lab.
Fort Belvoir, Virginia

Ballistics Research Labs. 2
Aberdeen Proving Ground
Maryland
Attn: D.W.H. Delsasso

Chief, Ordnance Develop. Div. 2
Natl. Bureau of Standards
Connecticut Av, VanNess St, NW
Washington 25, D. C.

Commanding Officer 1
Frankford Arsenal
Bridesburg, Philadelphia, Pa.

Thermionics Branch 5
Signal Corps Eng. Labs.
Evans Signal Lab, Bldg. 42
Belmar, New Jersey

Commanding General 1
Air Research and Dev. Command
ATTN: RDSBTL(Hq.Tech.Library)
Andrews Air Force Base
Washington 25, D. C.

Commanding General WCLC 1
Wright Air Devel.Center WCLRC 1
Wright-Patterson AF Base, Ohio

Commanding General CRRE 1
AF Cambridge Research Center
230 Albany Street
Cambridge 39, Massachusetts

Commanding General RCRW 1
Rome Air Development Center
Griffiss Air Force Base
Rome, New York

Commander 5
Armed Services Tech. Info.
ATTN; TIPDR
Arlington Hall Station
Arlington 12, Virginia

Director CR4582 1
Air University Library
Maxwell AF Base, Alabama

Chief, Western Division 1
Air Research and Devel.Command
Office of Scientific Research
P.O.Box 2035, Pasadena, Calif.

Microwave Laboratory 1
Stanford University
Stanford, California
Attn: F.V.L. Pindar

University of Michigan 1
Electron Tube Laboratory
Ann Arbor, Michigan
Attn: J. Rowe

Mr. John S. McCullough 1
Eitel-McCullough, Inc.
San Bruno, California

Johns Hopkins University 1
Radiation Laboratory
1315 St. Paul Street
Baltimore 2, Maryland
Attn: M. Poole, Librarian

Raytheon Corporation 1
Waltham, Massachusetts
Attn: Librarian

Cascade Research 1
53 Victory Lane
Los Gatos, California

Engineering Library 1
Stanford University
Stanford, California

Research Lab.of Electronics 1
Massachusetts Inst. of Tech.
Cambridge 39, Massachusetts

Sloane Physics Laboratory 1
Yale University
New Haven, Connecticut
Attn: R. Beringer

Mr. H. J. Reich 1
Department of Elec. Eng.
Yale University
New Haven, Connecticut

Electron Tube Section 1
Electrical Engineering Dept.
University of Illinois
Champaign, Illinois

Chairman, Div. of Elec. Eng. 1
University of California
Berkeley 4, California

Technical Report Collection 1
303A, Pierce Hall
Harvard University
Cambridge 38, Massachusetts

Laboratory for Insulation Res. 1
Massachusetts Inst. of Tech.
Cambridge 39, Massachusetts
Attn: A. von Hippel

Chief, West Coast Office 1
Signal Corps Eng. Labs.
75 So. Grand Avenue
Pasadena, 2, California

Periodicals Librarian 1
General Library
California Inst. of Technology

Lincoln Laboratory 1
Massachusetts Inst. of Tech.
Cambridge 39, Massachusetts

Signal Corps Resident Engineer 1
Electronic Defense Lab.
P.O. Box 205
Mountain View, California

Cornell Aeronautical Laboratory 1
Cornell Research Foundation
Buffalo 21, New York

Director, Electronics Defense 1
Engineering Research Inst.
University of Michigan
Ann Arbor, Michigan

Georgia Inst. of Technology 1
Atlanta, Georgia
Attn: Librarian

Fred D. Wilimek 1
Varian Associates
611 Hansen Way
Palo Alto, California

John Dyer 1
Airborne Instrument Laboratory
Mineola, L.I., New York

Bell Telephone Laboratories
Murray Hill, New Jersey
Attn: Librarian 1
J. R. Pierce 1

Hughes Aircraft Company 1
Culver City, California
Attn: Mr.Milek, Tech.Librarian

RCA Laboratories 1
Princeton, New Jersey
Attn: Mr.Herold and H.Johnson

Federal Tele. Laboratories
500 Washington Avenue
Nutley, New Jersey
Attn: W. Derrick 1
K. Wing 1

Technical Library 1
G.E. Microwave Laboratory
601 California Avenue
Palo Alto, California

Columbia Radiation Laboratory 1
538 W. 120th Street
New York 27, New York

Countermeasures Laboratory 1
Gilfillan Brothers, Inc
1815 Venice Boulevard
Los Angeles, California

The Rand Corporation 1
1700 Main Street
Santa Monica, California
Attn: Librarian

Technical Library 1
Research and Development Board
Pentagon Building
Washington 25, D. C.

Motorola Riverside Res. Lab. 1
8330 Indiana Avenue
Riverside, California
Attn: Mr. John Byrne

Chief, Bureau of Ships 816 1
Department of the Navy 820 1
Washington, D. C. 840 1

Advisory Group on Electron Tubes 1
346 Broadway (8th Floor)
New York 13, New York

Supervisor of Research Lab. 1
Electrical Engineering Bldg.
Purdue University
Lafayette, Indiana

W. E. Lear 1
University of Florida
Department of Electrical Eng.
Gainesville, Florida

Director, Microwave Res. Inst. 1
Polytechnic Inst. of Brooklyn
55 Johnson Street
Brooklyn 1, New York

Material Lab. Library, 912B 1
New York Naval Shipyard
Brooklyn 1, New York

University of Washington
Dept. of Electrical Engineering
Seattle, Washington
Attn: E. A. Harrison 1
A. V. Eastman 1

University of Colorado 1
Department of Elec. Engineering
Boulder, Colorado

Ramo-Wooldridge Corporation 1
Control Systems Division
P.O. Box 900B
Hawthorne, California
Attn: Librarian

Electrical Engineering Dept. 1
Princeton University
Princeton, New Jersey

National Union Radio Company 1
350 Scotland Road
Orange, New Jersey
Attn: Dr. A. M. Skellet

Dr. J. E. Shepherd 1
Sperry Gyroscope Company
Great Neck, L.I., New York

W. L. Maxson Corporation 1
460 West 34th Street
New York 1, New York
Attn: M. Simpson

Mr. H. R. Argento 1
Raytheon Corporation
Waltham, Massachusetts

Dr. E. D. McArthur 1
Electron Tube Laboratory
General Electric Company
Schenectady, New York

General Electric Company 1
Electronic Components Division
Power Tube Department
Microwave Lab. at Stanford
Palo Alto, California

Office of Technical Services 1
Department of Commerce
Washington 25, D. C.

Professor W. P. Dyke 1
Linfield College
McMinnville, Oregon

Stanford Electronics Labs. 1
Stanford University
Stanford, California
Attn: Electronics Lab.Library

Mr. E. C. Okress, Tech.Director 1
P.O. Box 284
Electronic Tube Division
Westinghouse Electric Corp.
Elmira, New York

Mr. Gilbert Kelton 1
Security Officer
Philips Laboratories
Irvington-on-Hudson, New York

University of Colorado 1
Engineering Experiment Sta.
Boulder, Colorado
Attn: W. G. Worcester

Dr. Z. Kaprielian 1
Electrical Engineering Dept.
University of Southern Calif.
Los Angeles 7, California

Dr. G. E. Barlow 1
Australian Joint Service Staff
Box 4837
Washington 8, D. C.

R. E. McGuire, Librarian 1
Office of the Director of Res.
Boeing Airplane Company
P.O. Box 3707
Seattle 24, Washington

Dr. Donald W. Kerst 1
General Atomic
P. O. Box 608,
San Diego, California

Image Instruments, Inc. 1
51 Waldorf Road
Newton Upper Falls 64, Mass.

Radiation Laboratory 1
Tech. Information Division
University of California
Berkeley 4, California